

 Open access • Journal Article • DOI:10.1179/174367508X306532

Synthesis and characterisation of bioactive and antibacterial glass–ceramic Part 1 – Microstructure, properties and biological behaviour — [Source link](#)

Enrica Verne, Sara Ferraris, Marta Miola, Giacomo Fucale ...+5 more authors

Institutions: Polytechnic University of Turin, University of Turin

Published on: 01 Oct 2008 - Advances in Applied Ceramics (Taylor & Francis)

Topics: Antibacterial agent, Bone regeneration, Biocompatibility and Glass-ceramic

Related papers:

- [How useful is SBF in predicting in vivo bone bioactivity](#)
- [Silver containing bioactive glasses prepared by molten salt ion-exchange](#)
- [Synthesis and characterisation of bioactive and antibacterial glass-ceramic Part 2 – plasma spray coatings on metallic substrates](#)
- [Surface silver-doping of biocompatible glass to induce antibacterial properties. Part I: Massive glass.](#)
- [Surface characterization of silver-doped bioactive glass.](#)

Share this paper:    

View more about this paper here: <https://typeset.io/papers/synthesis-and-characterisation-of-bioactive-and-xqvxw4rsxs>

AperTO - Archivio Istituzionale Open Access dell'Università di Torino

Synthesis and characterisation of bioactive and antibacterial glass-ceramic Part 1 - Microstructure, properties and biological behaviour

This is the author's manuscript

Original Citation:

Availability:

This version is available <http://hdl.handle.net/2318/44217> since

Published version:

DOI:10.1179/174367508X306532

Terms of use:

Open Access

Anyone can freely access the full text of works made available as "Open Access". Works made available under a Creative Commons license can be used according to the terms and conditions of said license. Use of all other works requires consent of the right holder (author or publisher) if not exempted from copyright protection by the applicable law.

(Article begins on next page)

Synthesis and characterisation of bioactive and antibacterial glass–ceramic Part 1 – Microstructure, properties and biological behaviour

E. Verné^{*1}, S. Ferraris¹, M. Miola¹, G. Fucale², G. Maina³, G. Martinasso⁴, R. A. Canuto⁴, S. Di Nunzio^{1,5} and C. Vitale-Brovarone¹

A glass–ceramic composition has been studied to realise a highly bioactive material, suitable for stimulate the bone regeneration, which has been subjected to a patented ion exchange process with silver ions, to impart antibacterial properties. The obtained material has been characterised by SEM, EDS and XRD analyses, before and after the introduction of Ag⁺ ions, and has been subjected to mechanical tests. Ag⁺ release was verified by GF-AAS analysis. The influence of silver on material wettability and bioactivity was evaluated through contact angle measurements and *in vitro* test on SBF solution. Finally, biocompatibility with osteoblast like cells and antibacterial test on *Staphylococcus Aureus*, have been realised to demonstrate the effective antimicrobial behaviour and the safety of silver doped glass–ceramic. On the basis of this study, it was evinced that ion exchange technique, optimised on glasses in previous research works, allows the controlled introduction of Ag⁺ ions and can be transferred on medical devices totally or partially realised with bioactive glass–ceramic.

Keywords: Glass-ceramic, Bioactive, Silver, Antibacterial, Ion exchange

Introduction

A typical problem connected with the implant of a medical device is the development of infections, due to bacteria adhesion and colonisation onto biomaterial surfaces. This situation often causes the failure of the implant and increases the hospital costs. Systemic antibiotic prophylaxis and special antiseptic operative procedures do not eliminate the infection rates, which range from 1 to 3% in total joint replacements.^{1,2} Bacteria compete with the cells of the body's immune system to colonise the surface of the implant. Moreover, the body's immune system is locally weakened by the presence of a foreign body and an injured bone. The production of extracellular biofilms on the surface of the implants often results in a very low efficacy of both body's immune system response and systemic prophylaxis. For these reasons, if bacteria colonise the surface

of the implant and its immediate surroundings, the possibility of developing an infection is very high. Thus, the use of implantable devices with an antibacterial surface, which starts releasing the active substance from the very first moment of implantation, represents a valid possibility to avoid bacterial colonisation and infections.

Silver, in the form of silver sulfadiazine, is one of the antibacterial agents utilised from years in different fields of medicine for the treatment of infections, particularly the ones associated with burns, because it shows a broad antibacterial behaviour.^{3,4} Even if a not negligible clinical cytotoxicity has been reported,^{5–8} silver is widely used in wound healing^{9,10} and in different biomaterials.^{11–14} This antimicrobial agent, in contrast to antibiotics, interferes with bacterial cells in different ways: it interacts with DNA and with proteins essential for bacterial respiration and transport of substances across cell membrane, inhibits the cell division and induces the rupture of cell membrane; for these reasons, the bacterial resistance is very limited. The activity of silver is defined as oligodynamic because at low concentration, the effect is interested in particular small prokaryotic cells (typically bacteria) while at higher concentration also eukaryotic cells are damaged. There is a range of silver concentration, defined as 'therapeutic window',¹⁴ which allows an antibacterial but not cytotoxic behaviour.

Lots of studies consider the use of silver to prevent prosthetic infection. The proposed solutions are

¹Department of Materials Science and Chemical Engineering, Politecnico di Torino, Torino, Italy

²Department of Chemical, Clinical and Microbiological Analyses CTO, Torino, Italy

³Department of Traumatology Orthopaedics and Occupational Medicine, Università di Torino, Torino, Italy

⁴Department of Experimental Medicine and Oncology, Università di Torino, Torino, Italy

⁵Present address: INSTM U.d.R Politecnico di Torino – LINCE Lab, Torino, Italy

*Corresponding author, email enrica.verne@polito.it

different: some authors realised coatings of pure metallic silver on stainless steel pins for orthopedic fixation¹⁵ and others introduced silver in the material composition,^{16,17} but the main difficulty remains in tailoring the amount of introduced silver in order to achieve an antibacterial behavior while maintaining biocompatibility.

Glasses and glass–ceramic with proper compositions in a well known compositional range,^{18,19} show biocompatibility and bioactive properties since they are able, by a complex mechanism involving ion leaching with the surrounding biological fluids, to induce the precipitation of hydroxyapatite on their surfaces. This layer of hydroxyapatite is considered as itself by the surrounding living tissues, thus its presence is widely recognised to be a sufficient requirement for the implant to bond with the living bone.^{20,21} These materials are widely studied and already used in different forms such as granules, bulk or coating materials in several applications where a chemical bond with the surrounding bone is highly required.^{22–27}

Silver containing bioactive glasses have been produced in different ways (melting and sol–gel):^{28–30} in order to produce silver containing bioactive glasses, the conventional meltquenching method is not effective to assure a reproducible silver ion distribution;³¹ this is the reason why up to date, only the sol–gel method has been proposed in literature for this purpose. However, the ionic diffusion in glasses can be successfully used aiming to modify their surface composition.³² The amount of silver introduced in material composition in bulk form is higher than that of the one added through a surface modification. On the other hand, the only useful silver is the one that could be released from surface in direct contact with injured tissues.

The aim of this work is to introduce a controlled and limited amount of silver on the surface of a bioactive glass–ceramic, to confer an antibacterial but not cytotoxic effect. For this purpose, the ion exchange technique, previously used to introduce silver in glasses of simple composition and low bioactivity index,^{33,34} was applied for the first time to a bioactive glass–ceramic of complex composition, aiming to develop, in an effective, quick and reproducible way, a new bone substitute able to promote both osteointegration and low infection risk.

Materials and methods

Synthesis of glass–ceramic

The material studied in this work is a glass–ceramic with the following molar composition: 50SiO₂–18CaO–9CaF₂–7Na₂O–7K₂O–6P₂O₅–3MgO. This composition belongs to a system in which the nucleation of fluorapatite is favourite^{35,36} and was chosen to obtain a bioactive glass–ceramic with ion exchange potentialities. The glass–ceramic, named Fa-GC from now on, was prepared by conventional melt and quenching route, followed by sintering at opportune conditions, in order to obtain a controlled and reproducible devitrification of the parent glass. The starting components have been melted in a platinum crucible at 1550°C for 1 h. Since the melt is prone to spontaneous and inhomogeneous devitrification during cooling, it was not poured in a mould, but quenched in cold water, in order to minimise this phenomenon. The obtained frit

was then milled and sieved down to a grain size of 30–75 µm.

Sintering process optimisation

The characteristic temperatures of the parent glass were identified by means of differential thermal analysis (DTA Netzsch 404S) and differential scanning calorimetry (Perkin-Elmer DSC 7) performed on the sieved powders. The linear shrinkage and the optimal sintering temperatures of the glass–ceramic were estimated by means of hot stage microscopy, in the temperature range between 25 and 1000°C on cubic green compacts of 3 × 3 × 3 mm in size.

The powders have been uniaxially pressed obtaining green compacts of 5 × 5 × 40 mm in size. The green compact have been subsequently sintered using different temperature and time schedules, chosen on the basis of the previous thermal analyses. After a preliminary characterisation of the sintered samples obtained in different conditions, the optimal sintering schedule has been individuated and used to produce samples for surface modification.

Characterisation of sintered samples

Structural analyses were performed by means of X-ray diffraction (X'Pert Philips diffractometer: Bragg–Brentano configuration and Cu K_α incident radiation), to identify the crystalline phases formed during sintering. The crystalline phases were observed also by scanning electron microscopy (SEM Philips 525M) on chemically etched sintered samples and analysed by EDS (Philips, EDAX 9100).

The sintered glass–ceramic has been subjected to a complete mechanical characterisation: the Young's modulus was evaluated by means of acoustic method (Grindosonic) on sintered bars and the Vickers indentations were performed to estimate the hardness (HV) and the fracture toughness (*K_{IC}*) of the glass–ceramic, using a load of 10 kg and the following equation

$$HV = 2F \frac{\sin(136^\circ/2)}{l^2} = 1854 \left(\frac{F}{l^2} \right)$$

$$K_{IC} = 0.016(E/HV)^{1/2}(P/c^{3/2})$$

where *F* and *P* are the load applied, *l* is the diagonals mean of the mark, *E* is the Young's modulus and *c* is the crack length. Before the hardness test, the samples were polished with 1 µm diamond paste.

To verify the material strength, flexural tests with three and four points bend loading geometry (dimensions: 52 × 10 × 4 mm) were performed. The flexural strength was calculated from the standard equation

$$\sigma = \frac{3 Fl}{2 b^2 a}$$

where *F* is the applied load, *l* is the distance between the supports, and *a* and *b* are the parameters of the section. The maxima inflexion was valuated using the following equation

$$\eta_{\max} = \frac{Fl^3}{24EJ}$$

where *E* is the glass–ceramic elastic modulus and *J* is the inertia of the section.

Surface modification

To introduce silver inside the glass–ceramic, an ion exchange process has been selected. This technique focuses particularly on the amorphous phase of the material and is based on the exchange of modifier cations (especially Na^+ ions) with silver ions of the solution.^{33,34} This process allows the introduction of silver ions only in the outer layers of the samples, maintaining unaltered bulk characteristics, such as mechanical properties and bioactivity.

In this work, the ion exchange process was performed in aqueous solution of silver nitrate, following a protocol described elsewhere.³⁷ Samples modified by this technique will be named Ag-GC from now on.

The samples were analysed by means of X-ray diffraction, SEM and EDS to evaluate the modification induced by the ion exchange process.

In vitro bioactivity

In order to evaluate bioactive behaviour of both unmodified glass–ceramic and Ag-GC, samples were soaked in simulated body fluid (SBF) for up to 1 month at 37°C. A refresh of the solution was made every 2 days to mimic physiological turnover of body fluids; at the same time, the pH of the solution was monitored. The SBF used in this work is the one proposed by Kokubo and it mimics the inorganic salt composition of human physiological fluids.^{18–20,38}

Wettability

Surface wettability was determined by measurement of static contact angle with water, before and after ion exchange process, to verify the eventual modifications due to the presence of silver.

Water was used because the biological fluids are composed in the greater part by water and the test was performed because the hydrophobic/hydrophilic behaviour is significant in the cellular tests, as research works in literature confirm^{39,40} that bacteria preferentially adhere on hydrophilic surfaces rather than on hydrophobic ones.

Leaching tests

The amount of released silver ions was investigated by soaking Ag-GC samples in SBF for up to 1 month at 37°C without refreshing. Graphite furnace-atomic adsorption spectrophotometry (GF-AAS, Perkin-Elmer 4100 ZL) analyses were performed in 1 mL SBF spiked from the soaking solution after 3 h and 1, 3, 7, 14 and 28 days dipping. The leaching tests were performed in triplicate and for comparative purposes, also one unmodified glass–ceramic with the same dimensions, was tested.

Biocompatibility tests

Since Ag-GC is intended for bone tissue integration, biocompatibility and cytotoxicity tests were carried out on human osteoblast-like cells (MG-63). Samples of as sintered Fa-GC and of Ag-GC were soaked in minimum essential medium (M5650 Sigma) added with 1 mM sodium pyruvate, 1% antibiotics and antimycotics solutions, 2 mM glutamine and 10% serum. After 24 h, 10 000 cells/cm² were seeded on samples and maintained for 2, 4 and 8 days at 37°C in the atmosphere of 5%CO₂ and 95% air. Tests were performed, at each time, part on cells (optical

microscope observation, count, SEM observation) and part on the supernatant (pH and lactate dehydrogenase measurements). All tests were performed in triplicate.

Optical microscope observation describes the presence and morphology of cells around the sample and is a qualitative index of material's biocompatibility. Vital count, performed using trypan blue colorant, is a quantitative index of cells' vitality in the presence of Fa-GC and Ag-GC.

In order to evaluate the presence and the morphology of cells on samples surface, specimens were fixed and observed by SEM. pH is a measure of cellular metabolic activity, and in particular medium's acidification shows good cell's metabolism. The presence of lactate dehydrogenase (LDH) is an index of cellular death for necrosis. Lactate dehydrogenase (LDH) is measured by spectrophotometry.

Antibacterial tests

Two kinds of microbiological tests have been performed in accordance to NCCLS standards for antimicrobial susceptibility: inhibition zone evaluation⁴¹ and broth dilution tests.⁴² All products for this analysis have been purchased from BD-Becton Dickinson.

In both cases, a bacterial broth has been prepared dissolving a *S. Aureus* disc (ATCC 29213) in 5 mL brain heart infusion. After overnight incubation at 37°C, 10 µL suspension has been spread on a blood agar plate and incubated for 24 h. A 0.5 McFarland suspension (containing approximately $1-2 \times 10^8$ CFU mL⁻¹) has been prepared inoculating some colonies grown on the plate in physiological solution (turbidity has been evaluated by optical instrument, Phoenix Spec BD McFarland)

In order to carry out inhibition zone evaluation, an aliquot of the described suspension has been spread on Mueller–Hinton agar plates on which samples have then been posed with the treated surface in contact with plate. After 24 h incubation, inhibition zones have been observed as a halo around samples where bacteria did not grown up.

In order to perform dilution tests, an aliquot of bacterial suspension has been introduced in Mueller–Hinton broth tubes in order to obtain suspensions containing $\sim 5 \times 10^5$ CFU mL⁻¹.

A tube containing only bacteria has been prepared as growth control, and in the other tubes, samples and silver containing samples have been introduced.

After 24 h incubation at 35°C, tubes' turbidity has been optically evaluated (Phoenix Spec BD McFarland).

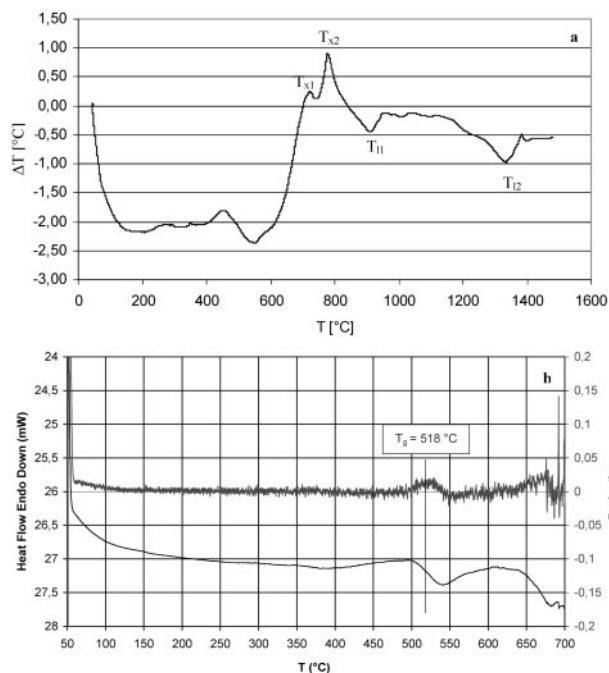
As for samples broth, washing and vortexing solutions have been analysed in order to quantify colony forming units (CFU). The washing solution has been prepared by rapid rinsing of sample in physiological solution, while the vortexing one is prepared by 1 min 50 Hz vortex of sample in physiological solution.

Each solution has been serially diluted and spread on blood agar plates. After overnight incubation at 35°C, CFU have been counted on plates. Each test has been carried out in triplicate.

Results and discussion

Thermal analyses

Thermal analyses (DTA and DSC) allow the identification of the material characteristic temperatures: glass



1 Thermal analysis diagrams of a DTA and b DSC (upper curve is derivative) on Fa-GC

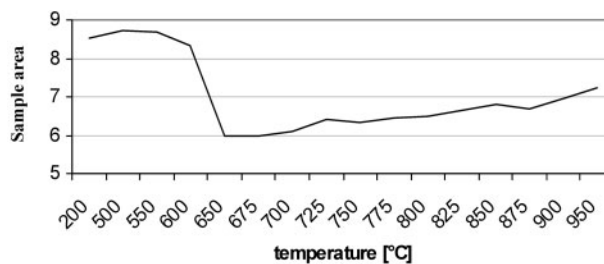
transition temperature T_g , crystallisation temperature T_x and liquidus temperature T_l . The diagrams (Fig. 1) have shown two exothermic crystallisation peaks at 730 and 780°C, related to two crystalline phases; the onset temperature of the first peak is 620°C.

The liquid temperatures of the two crystalline phases have been identified at 900 and 1310°C and the glass transition temperature T_g is 518°C.

To investigate the shrinkage of the green compacts and the influence of the two crystallisation phenomena on this step, a dilatometric analysis was performed, by means of hot stage microscopy from room temperature to 1000°C. Figure 2 shows the graphs relative to hot stage microscopy in the temperature range 200–1000°C: at 500°C, the sample expands slightly; between 550 and 625°C, it become to shrink; this behaviour is due to viscous flowing of the amorphous phase and initial sintering. From 675 to 850°C, a range in which two crystallisation processes are occurring, the sample starts again to expand and finally at higher temperature, the softening begins.

The optimal sintering temperatures were chosen on the basis of the thermal analyses. The green bars were sintered at 650 and 800°C, i.e. the temperature of the maximum shrinkage, and for comparison purposes, the nearer temperature to the liquid phase formation respectively. The samples were initially sintered for 3 h, then, after SEM observation and density estimation, the sintering time was reduced to 1 h.

As expected, XRD phase analysis shows that the as prepared glass contains a little amount of apatite (probably fluorapatite, due to the composition of the glass) in the amorphous matrix (Fig. 3a). After the thermal treatment, both at 650 and 800°C, fluorapatite signals grow in a significant way, and another crystalline phase, identified as canasite, is detected (Fig. 3b and c). These results agree with thermal analyses and demonstrate that crystalline phases are present only in few amounts immediately after the pouring and increase



2 Linear shrinkage of Fa-GC green compact

during the thermal treatments. No other crystalline phase appears in this process. Scanning electron microscopy (SEM) and EDS observations demonstrate the presence of the two phases (Fig. 4).

Mechanical tests

Vickers indentations were performed on a set of three Fa-GC specimens sintered at the two chosen temperatures, to study the cracks propagation and hardness. Vickers hardness measured on samples sintered at 650°C is higher than that measured on samples sintered at 800°C ($HV_{650} = 5.62 \pm 0.66 \text{ GN m}^{-2}$; $HV_{800} = 4.67 \pm 1.55 \text{ GN m}^{-2}$). This feature is probably due to the expansion occurred above 650°C, which causes a lower density of samples sintered at 800°C that compromises the mechanical properties. For this reason, a complete mechanical characterisation was performed only Fa-GC bars sintered at 650°C.

The calculated fractures toughness was about $0.92 \pm 0.08 \text{ MPa m}^{-1}$, a value comparable with other data found in literature for glass-ceramics used in odontology.⁴³ The elastic modulus, valued by means of acoustic method, is 54 GPa.

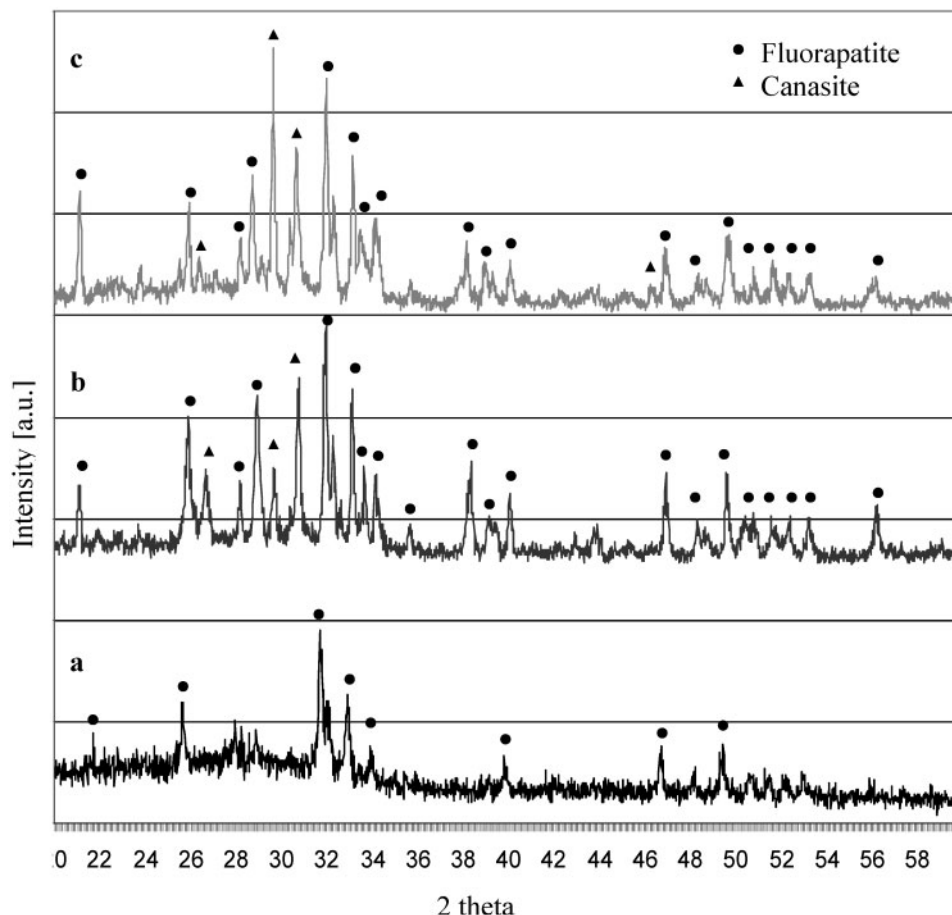
The flexural strength was $68 \pm 6 \text{ MPa}$ for three points flexure and $72 \pm 6 \text{ MPa}$ for four points flexure; these results are interesting, because the human bone flexural strength is included between 49 and 180 MPa.^{44,45}

On the basis of these results, surface modification of Fa-GC and its further characterisations, were performed only on samples sintered at 650°C for 1 h.

Surface modification

The aim of this research is the realisation of an antibacterial surface able to reduce the bacterial adhesion and proliferation, without compromising substrate properties, such as biocompatibility and mechanical resistance. In order that a medical device has antimicrobial properties, it is necessary to produce an antibacterial surface, which is the device portion that comes in contact with human body, fluids, tissues, cells and also bacteria. For this reason, it is not essential to impart antibacterial properties to the substrate; moreover, silver ions coming from the internal bulk could be trapped and accumulated between the implant and the new formed tissue, causing toxic effect or the argyria.

Ion exchange technique allows the introduction of silver ions only in the upper atomic layers of the material, which is demonstrated by EDS analysis at different voltages. In this way, a qualitative diffusion profile of silver in sample's depth was realised, as shown in Fig. 5. As demonstrate in previously researches,^{33,34} the patented process permits to control and tune the amount of silver introduced varying process parameters, in function of material composition. In particular, the



3 XRD patterns of Fa-GC at a 25°C, and after thermal treatment at b 650 and c 800°C

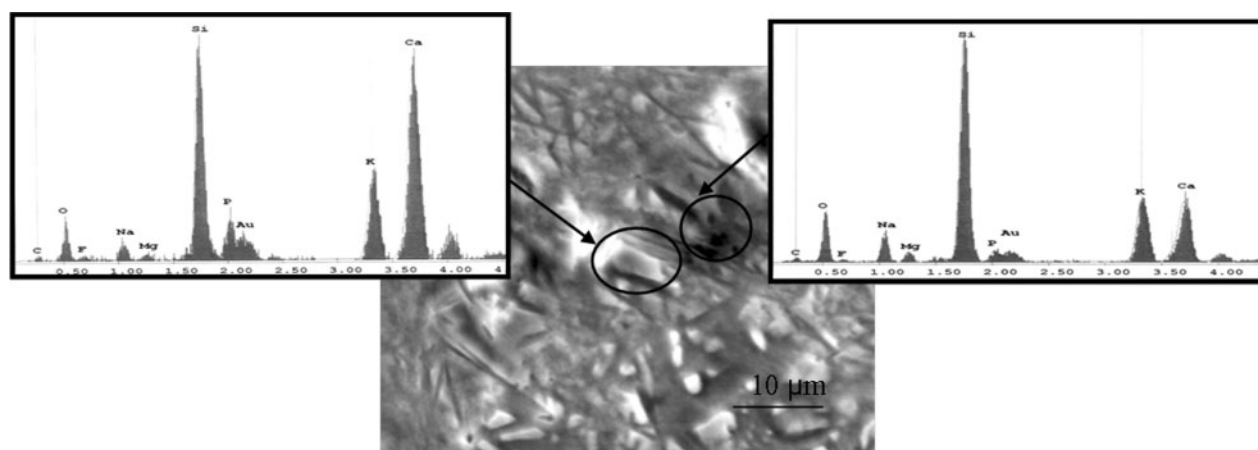
ion exchange parameters allow modulating the thickness depth of silver doped layer and to realise a thin layer containing Ag^+ ions, thus obtaining an immediate release and maintaining the bulk characteristics unchanged.

X-ray diffraction (XRD) analyses, before and after ion exchange process, show that no new crystalline phase grows during the treatment (Fig. 6). This means that silver ions entered into the network of the residual amorphous phase of Fa-GC without uncontrolled reactions, such as, for example, the formation of silver phosphates. Moreover, the amount of introduced silver and the process conditions did not induce the reduction

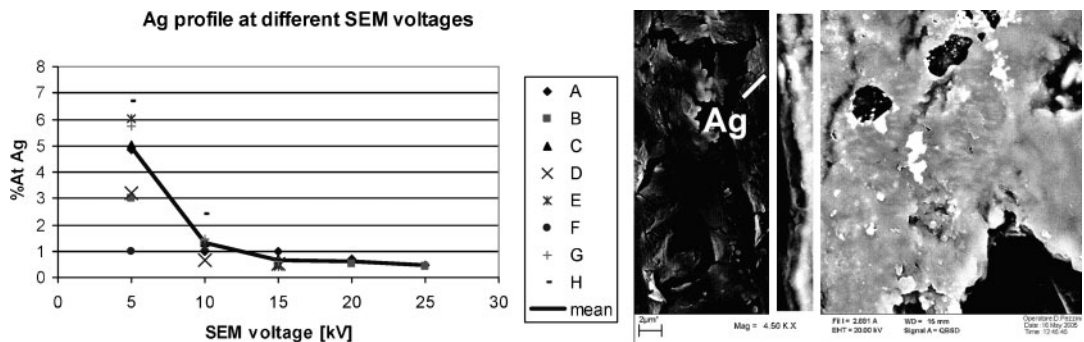
of silver ions to metallic silver clusters, at least how far was detectable by conventional XRD.

Sample's morphology is maintained after treatment, as observed by SEM. Analysis by EDS shows the appearance of small silver's peak; the amount of quantified silver by EDS is included in the instrument error limits (Fig. 7).

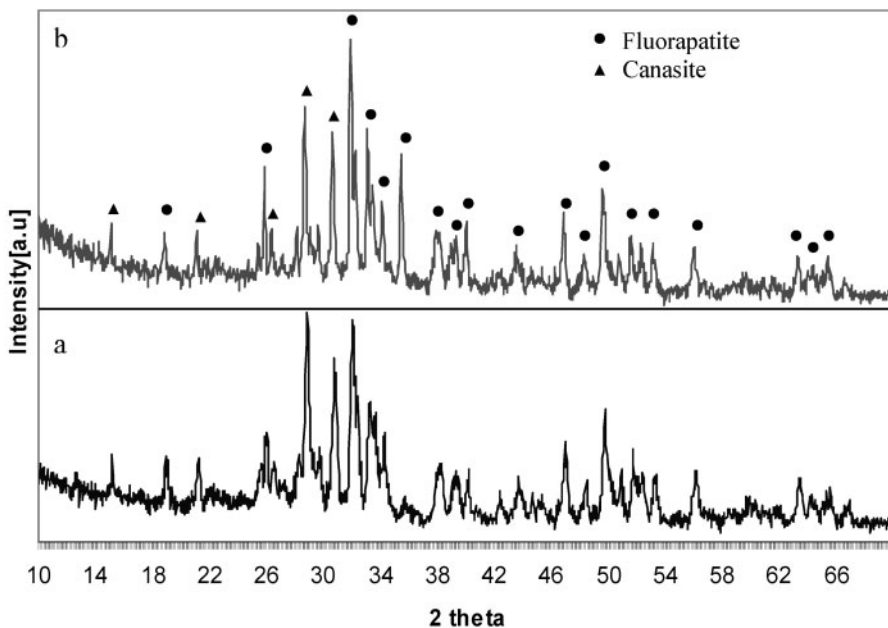
Weights of samples have been measured before and after ion exchange process, and no variations are observed (Table 1), indicating that the treatment does not induce any dissolution phenomena and that the limited amount of introduced silver is not detectable through this measurement, as on the contrary, realised



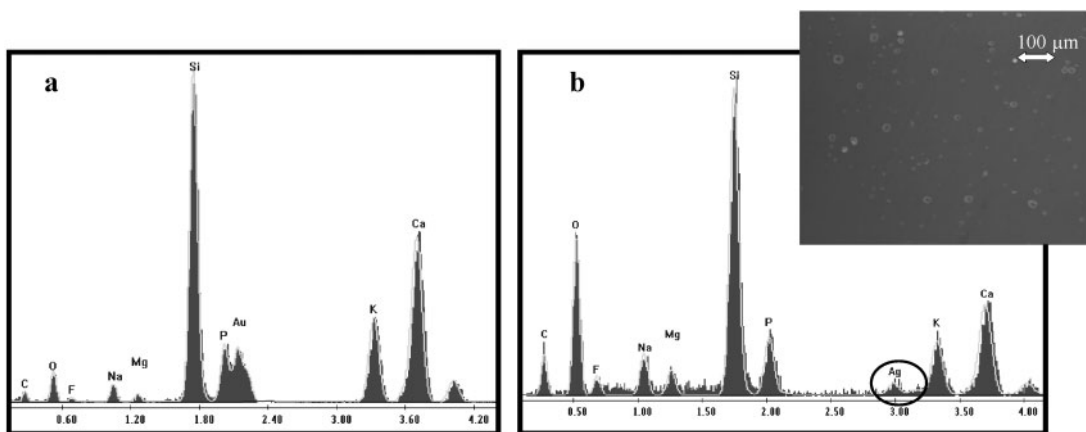
4 SEM and EDS analyses of Fa-GC show presence of two crystalline phases



5 Ag profile and SEM image with modified layer underlined in box



6 XRD spectra of a GC and b Ag-GC



7 EDS analyses a before and b after ion exchange process, including SEM image

in the previous work.³³ The results are in accordance to SEM observations.

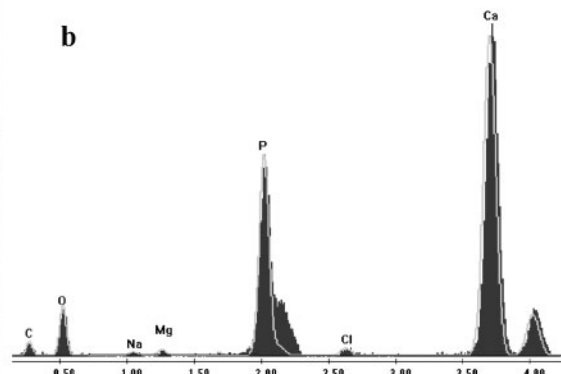
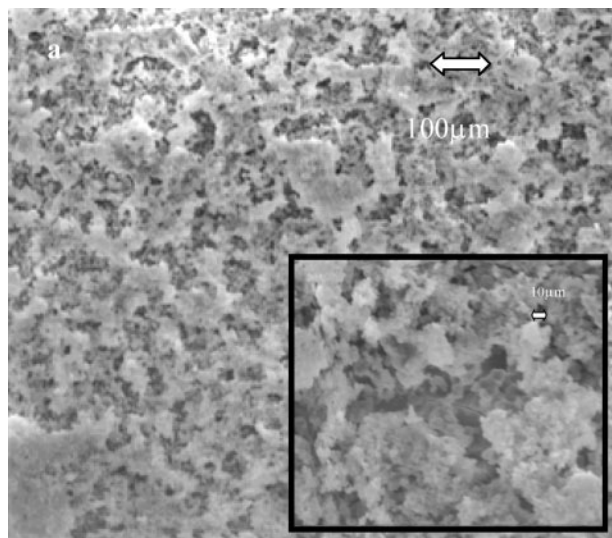
In vitro tests

In order to evaluate the bioactivity of the glass–ceramic before and after ion exchange process, samples soaked in SBF for up to 1 month, were analysed by XRD and observed by SEM. After 14 day dipping, XRD patterns

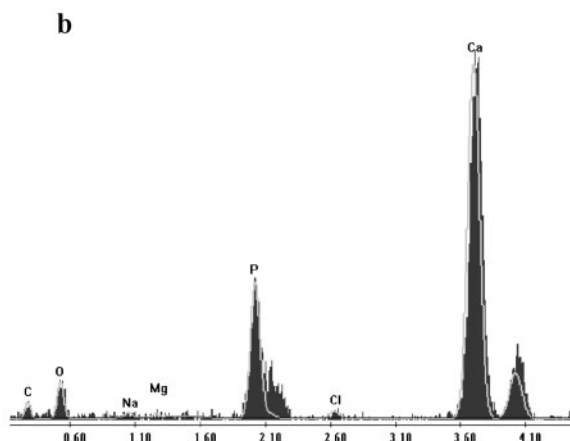
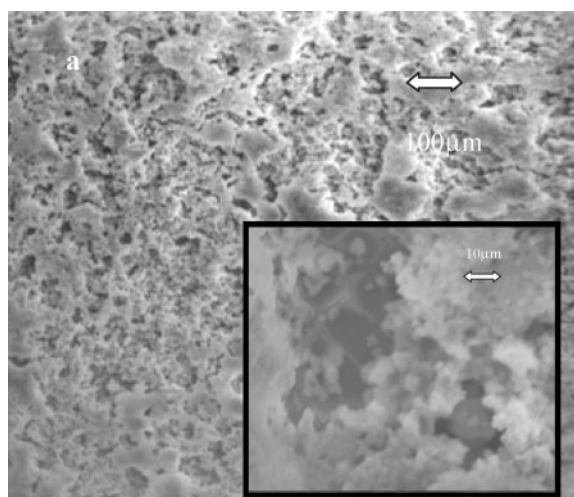
indicate the formation of a hydroxyapatite layer (HAp) on both surfaces of Fa-GC and Ag-GC samples. Scanning electron microscopy (SEM) images show the

Table 1 Weight of sample before and after ion exchange

	Initial weight, g	Final weight, g
Mean	0.3106	0.3102
Standard deviation	0.0072	0.0073



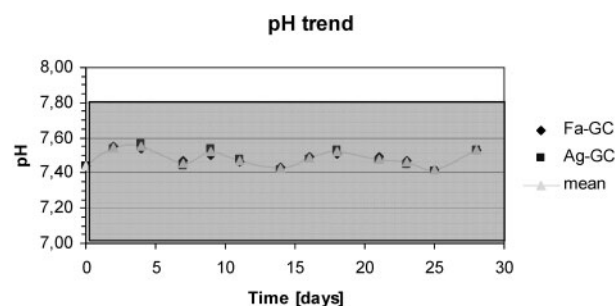
a SEM image; b EDS spectrum
8 HAp on Fa-GC after 14 days in SBF



a SEM image; b EDS spectrum
9 HAp on Ag-Fa-GC after 14 days in SBF

presence of uniform layer of a substance with the typical globular morphology of HAp, and EDS analysis confirms the enrichment in Ca and P for both samples (Figs. 8 and 9). This result indicates that Fa-GC is a bioactive glass–ceramic³⁸ and that silver introduction by ion exchange technique does not affect material’s bioactive behaviour.

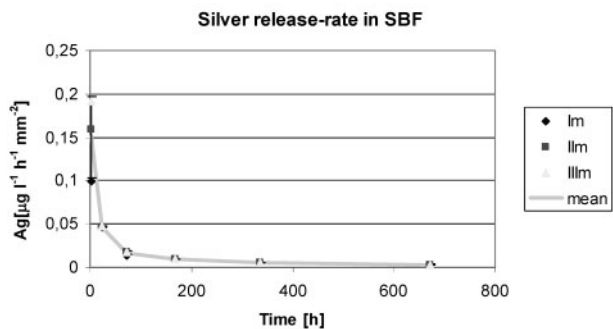
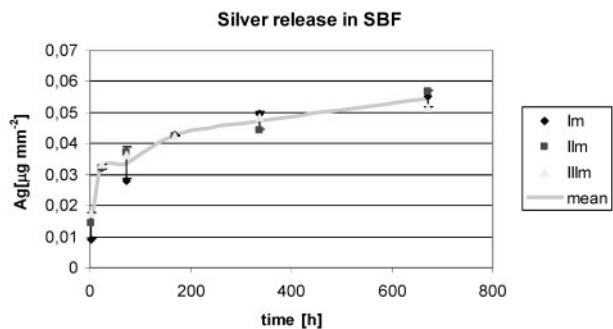
The trend of pH during the dipping period shows little variations, in accordance to physiological values. The most critical tissue as for pH variation tolerability is blood, its pH must be quite constant around the value of 7.4 (7.35–7.45) and the maximum variations tolerated are in the range 7.0–7.8. Typical pH for human tissular cells is around 6.9. Figure 10 shows pH trend for Fa-GC and Ag-GC, and pH tolerability range for blood, any difference was observed in pH trend between Fa-GC and Ag-GC. Then, even the silver is introduced on glass–ceramic surface, it does not interfere with bioactivity process mechanisms that really involve materials surface; it is very interesting to realise a device both antibacterial and bioactive, which promotes the osteointegration through the formation of apatite layer on its surface.



10 pH trend and physiological tolerability range (in box)

Leaching test

In order to quantify the amount of silver released in solution from the doped glass–ceramic, eluates of Ag-GC, soaked in SBF, were analysed at different soaking times by GF-AAS technique. Figure 11 shows the amount of silver in solution, expressed in $\mu\text{g mm}^{-2}$, and leaching speed, expressed in $\mu\text{g l h mm}^{-2}$.



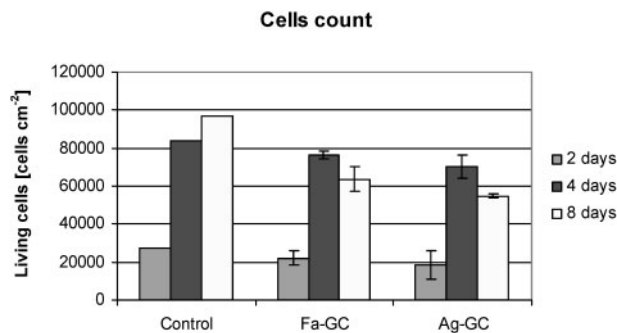
11 Silver release amount and rate

The leaching trend demonstrates that silver, introduced in the glass-ceramic by ion exchange, is gradually released in SBF and particularly in the first period, which is the most critical for infections' development.^{33,34}

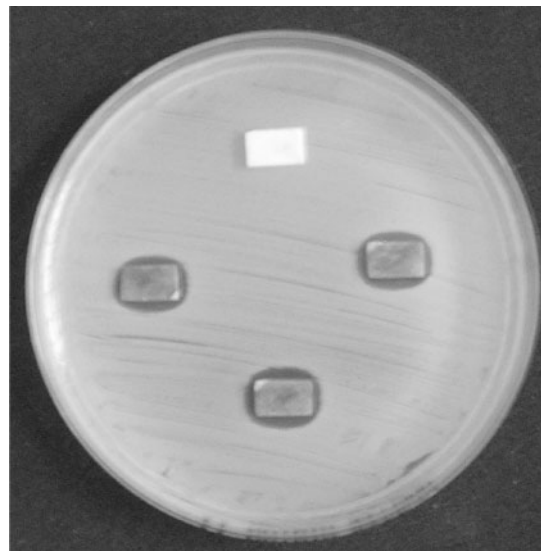
The leaching curve show a little decrease around 24–72 hours of release. This trend is probably due to the precipitation of small amount of AgCl^{33,34} on samples' surfaces soaked in SBF for less than 14 days, as confirmed by SEM observation. The silver release is performed in SBF, a solution rich in ions, in particular phosphates, being able to complex silver ions and increase the AgCl solubility. However, phosphates are attracted by calcium ions, also present in great amount in SBF; they precipitate as calcium phosphate and crystallise as HAp on glass-ceramic surface during the bioactivity process. Then, the solution is depleted in phosphates and silver can precipitate as AgCl on samples' surfaces; for this reason, the amount of silver in the solution decreases slowly during the leaching test.

Wettability test

Wettability measurements gave a mean static contact angle of 65° for Fa-GC and of 72° for Ag-Fa-GC. According to these values, ion exchanged samples are a little more hydrophilic than simple glass-ceramic ($p < 0.05$). This can be explained by observation that



13 Osteoblast's viable count on control, Fa-GC and Ag-GC



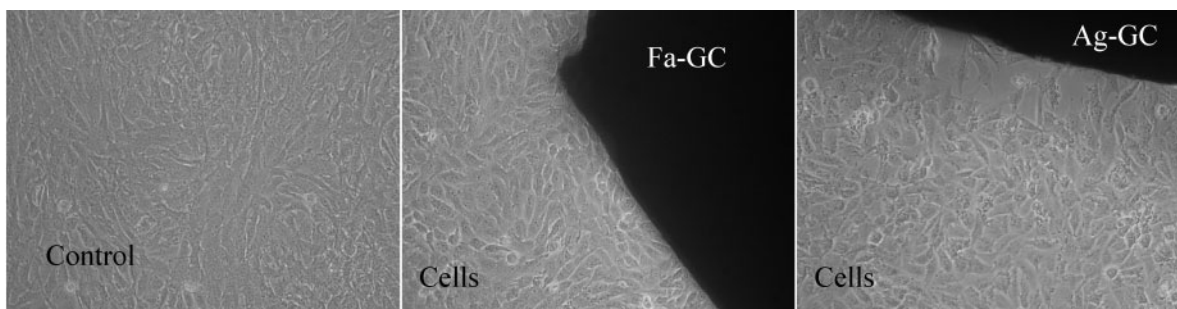
14 Inhibition zone evaluation: top of plate: Fa-GC sample; below: three Ag-GC samples

before ion exchange process, the glass-ceramic surface is first characterised by O–Na bonds, while after the treatment, O–Ag bonds are introduced. O–Na bond is more polar than O–Ag bond, so water molecules present a stronger attraction for an O–Na rich surface, which makes them a little more hydrophilic.

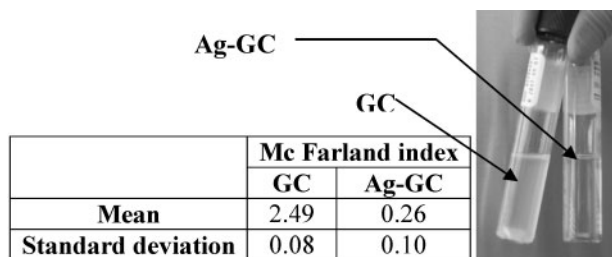
Since many bacteria adhere preferably to hydrophilic surfaces,^{39,40} the realisation of a more hydrophilic surface can be an added power to the antibacterial behaviour of silver to reduce the bacterial adhesion on glass-ceramic.

Biocompatibility tests

Figure 12 reports some optical micrographs of osteoblasts after 4 day culture and shows a comparison



12 Optical observation after 4 day culture



15 McFarland index

among a control, Fa-GC and Ag-GC. All images are similar in cell morphology. The presence of a substantial number of cells, which create a carpet on the culture surface even for Fa-GC and Ag-GC, is an index of material's biocompatibility in both treated and untreated forms. Viable count shows similar values for control, Fa-GC and Ag-Fa-GC cultures after 2 days (Fig. 13). The number of osteoblast in the samples after 8 days is lower in comparison with that of control, and it is also slightly lower in comparison with the value after 4 days. The last observation is due probably to the beginning of bioactivity process and the subsequently ions release by glass-ceramic in culture medium. So the viable count tests in both samples confirm that the amount of introduced and as a consequence, released silver does not influence significantly osteoblast's adhesion and proliferation.

pH value is 8.37 for basal medium. Table 2 shows pH mean values for control, Fa-GC and Ag-GC; an acidification after cell culture indicates active cellular metabolism. There are not substantial differences among control, treated and untreated samples.

The production of LDH in culture medium increases with culture time for both samples, in particular for Ag-GC samples after 8 days. The increase in LDH in both samples in comparison with the control can be due to ions (Na^+) coming from the glass during bioactivity process and ions and Ag^+ released respectively in untreated and treated samples. The ions and Ag^+ are accumulated in medium and interfere with cell vitality, since culture medium was not substituted during the 8 days of culture. On the contrary, in the human body, a process of clearance occurs: body fluids remove and clear the

Table 2 pH and LDH values

	pH			LDH		
	2 days	4 days	8 days	2 days	4 days	8 days
Control	8.12	7.98	8.23	48.76	42.35	67
Fa-GC	7.97	7.88	7.77	34.4	2.64	295.5
Ag-GC	8.00	7.87	7.71	0	0	546

products released from implant devices, inhibiting their accumulation.

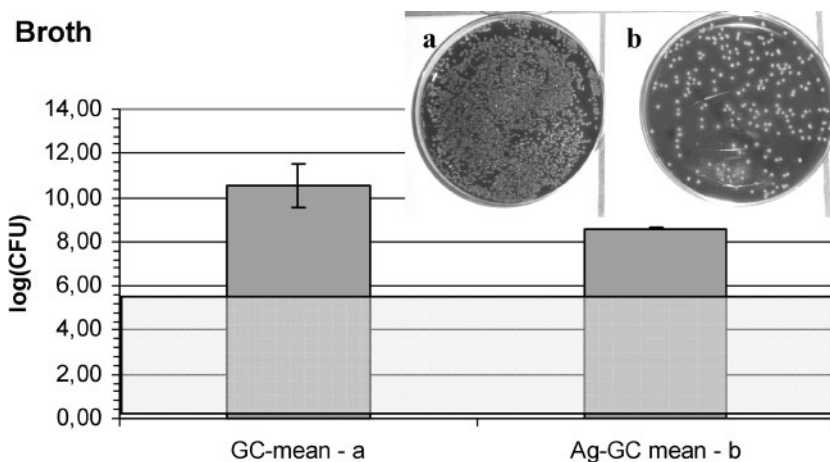
Antibacterial tests

The inhibition zone evaluation tests demonstrate the effective antibacterial properties of silver ions: Ag-GC samples are able to produce a significant and reproducible inhibition zone of growing bacteria, while the bacteria colonies grown all around the Fa-GC untreated specimens, tested as control (Fig. 14).

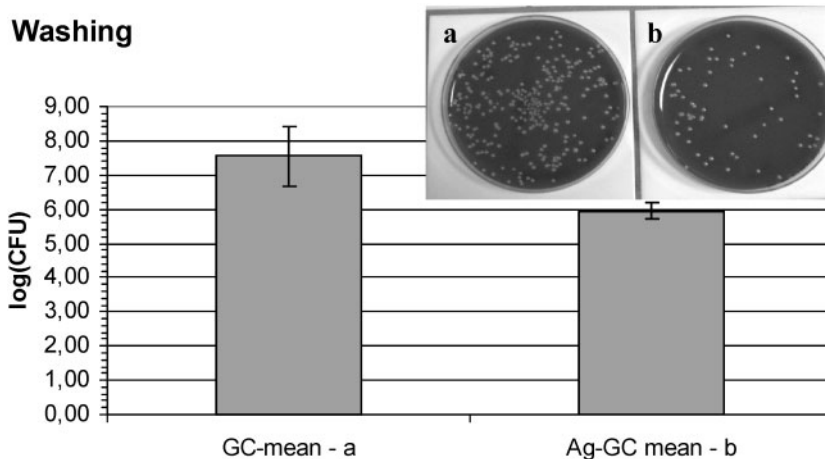
Quantitative information about antibacterial behaviour of silver doped samples is given by broth dilution tests. The first information is given by McFarland index, which is a measurement of broth turbidity: an increase in turbidity is due to bacterial proliferation. Figure 15 shows that silver containing samples present a significantly lower McFarland index (and a more limpid solution) than GC ones.

Solution analysis describes bacterial proliferation in the whole medium where both bacteria and samples have been incubated. Washing solution quantifies bacterial proliferation in the liquid film just around the sample, while vortexing solution determines the amount of bacteria adhered on samples' surfaces and detached by vortex treatment.

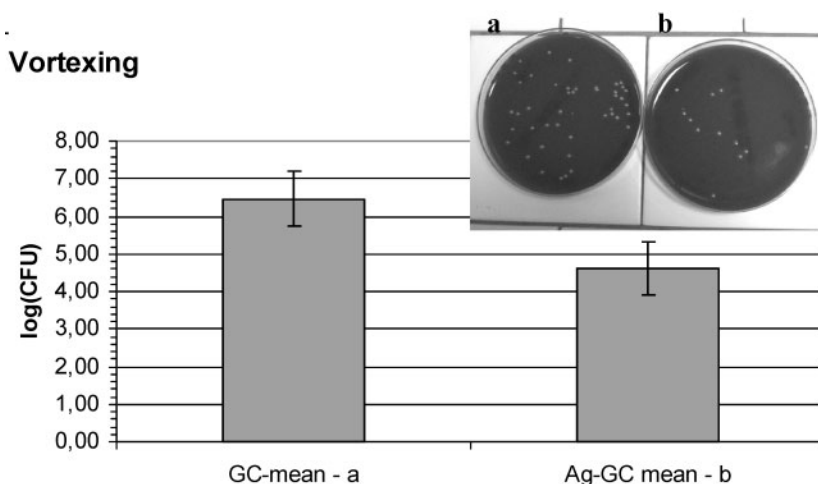
Broth and washing solutions present a reduction of almost three orders of magnitude for silver containing samples. The box in Fig. 16 underlines the amount of initial bacterial inoculum (Figs. 16 and 17). In the vortexing solution, a reduction of two orders of magnitude for treated samples is shown (Fig. 18). A reduction of CFU adhered on surfaces of samples is particularly significant since adhered bacteria cause the effective infection and often lead to a biofilm formation, i.e. a slime bacteria containing surface hardly penetrated by common antibiotics which is usually adopted to treat infections.



16 CFU count for broth



17 CFU count for washing solution



18 CFU count for vortexing solution

Conclusions

The ion exchange technique, already experimented on glass substrates, permits the introduction of low and controlled amount of silver without modifying bulk characteristics of bioactive glass–ceramic. The released amount of silver detected by GF-AAS is lower than those reported in literature for cytotoxic effect.

The material biocompatibility was confirmed also by biological tests: osteoblast like cells adhere and proliferate on both untreated and ion exchanged samples; therefore, the introduced and released silver does not cause cytotoxic effect, but confers only antimicrobial activity toward *S. Aureus*, the most common bacterial species that occurs in post-surgical infections.

This work confirmed that ion exchange method can be applied to different and complex glass and glass–ceramic compositions. It is extremely important to modify process parameters, to introduce and release controlled silver amounts (below clinical tolerance levels), and to verify cytotoxic effect before antibacterial activity is attested.

Coming efforts will be focused on the translation of this technique to glass–ceramic coated metallic devices, such as external fixation implants, or bone substitutes.

Acknowledgements

The authors would like to acknowledge Regione Piemonte (Italy) that partially funded this research

activity. V. Bergo and P. Spinelli (Traumatology Orthopaedics and Occupational Medicine Department, University of Turin, Turin, Italy) are kindly acknowledged for technical support.

References

1. I. Antti-Poika, G. Josefsson, Y. Kontinen, L. Lidgren, S. Santavirta and L. Sanzen: *Acta Orthop. Scand.*, 1990, **61**, 163–169.
2. W. H. Harris and C. B. Sledge: *N. Engl. J. Med.*, 1990, **323**, 801–807.
3. D. Wyatt, D. N. McGowan and M. P. Najarian: *J. Trauma*, 1990, **30**, 857–865.
4. C. S. Chu, A. T. McManus, B. A. Pruitt and A. D. Mason: *J. Trauma*, 1988, **28**, 1488–1492.
5. G. D. DiVincenzo, C. J. Giordano and L. S. Schiever: *Int. Arch. Occup. Environ. Health*, 1985, **56**, 205–215.
6. E. L. Jensen, J. Rungby, J. C. Hansen, E. Schmidt, B. Pedersen and R. Dahl: *Hum. Toxicol.*, 1988, **7**, 535–540.
7. A. P. Moss, A. Sugar, N. A. Hargett, A. Atkin, M. Wolkstein and K. D. Roseman: *Arch. Ophthalmol.*, 1979, **97**, 906–908.
8. K. D. Rosenman, A. Moss and S. Kon: *J. Occup. Med.*, 1979, **21**, 430–435.
9. E. A. Deitch, A. Marin, V. Malakanov and J. A. Albright: *J. Trauma*, 1987, **27**, 301–304.
10. H. W. Margraff and T. H. Covey: *Arch. Surg.*, 1977, **112**, 699–704.
11. T. Bechert, P. Steinrücke and J. P. Guggenbichler: *Nat. Med.*, 2000, **6**, 1053–1056.
12. T. Bechert, M. Böswald, S. Lugauer, A. Regenfus, J. Greil and J. P. Guggenbichler: *Infection*, 1999, **27**, S24–S29.
13. R. M. Joyce-Wöhrmann and H. Münstedt: *Infection*, 1999, **27**, S46–48.

14. V. Alt, T. Bechert, P. Steinrücke, M. Wagener, P. Seidel, E. Dingeldein, E. Domann and R. Schnettler: *Biomaterials*, 2004, **25**, 4383–4391.
15. A. Massè, A. Bruno, M. Bosetti, A. Biasibetti, M. Cannas and P. Gallinaro: *J. Biomed. Mater. Res. (Appl. Biomater.)*, 2000, **53**, 600–604.
16. M. Bellantone, N. J. Coleman and L. L. Hench: *J. Biomed. Mater. Res.*, 2000, **51**, 484–490.
17. M. Bellantone, N. J. Coleman and L. L. Hench: *Key Eng. Mater.*, 2001, **597**, 192–195.
18. A. Saranti, I. Koutselas and M. A. Karakassides: *J. Non-Cryst. Solids*, 2006, **352**, 390–398.
19. I. Barrios de Arenas, C. Schattner and M. Vasquez: *Ceram. Int.*, 2006, **32**, 515–520.
20. L. L. Hench: *J. Am. Ceram. Soc.*, 1993, **81**, 1705–1728.
21. W. Cao and L. L. Hench: *Ceram. Int.*, 1996, **22**, 493–507.
22. E. Verné, R. de Filippi, C. Vitale Brovarone, G. Karl and J. Vogel: *Mater. Med. Eng.*, 2000, **2**, 146–151.
23. E. Verné, C. Vitale Brovarone and D. Milanese: *J. Biomed. Mater. Res. (Appl. Biomater.)*, 2000, **53**, 408–413.
24. E. Verné, C. Vitale Brovarone, C. Moiescu, E. Ghisolfi and E. Marmo: *Acta Mater.*, 2000, **48**, 4667–4671.
25. E. Verné, E. Bona, A. Bellosi, C. Vitale Brovarone and P. Appendino: *J. Mater. Sci.*, 2001, **36**, 2801–2807.
26. C. Vitale Brovarone, E. Verné, A. Krajewski and A. Ravaglioli: *J. Eur. Ceram. Soc.*, 2001, **21**, 2855–2862.
27. E. Verné, M. Bosetti, C. Vitale Brovarone, C. Moiescu, F. Lupo, S. Spriano and M. Cannas: *Biomaterials*, 2002, **23**, 3395–3403.
28. M. Kawashita, S. Tsuneyama, F. Miyaji, T. Kokubo, H. Kozuka and K. Yamamoto: *Biomaterials*, 2000, **21**, 393–398.
29. M. Bellantone, L. L. Hench, S. Giannini and A. Moroni: *Bioceram. Key Eng. Mater.*, 2001, **192–195**, 617–620.
30. M. Bellantone, N. J. Coleman and L. Hench: *J. Biomed. Mater. Res.*, 2000, **51**, 484–490.
31. P. W. Wang, L. Zhang and Y. Tao: *J. Am. Ceram. Soc.*, 1997, **80**, 2285–2293.
32. R. Terai and R. Hayami: *J. Non-Cryst. Solids*, 1975, **18**, 217–264.
33. S. Di Nunzio, C. Vitale Brovarone, S. Spriano, D. Milanese, E. Verné, V. Bergo, G. Maina and P. Spinelli: *J. Eur. Ceram. Soc.*, 2004, **24**, 2935–2942.
34. E. Verné, S. Di Nunzio, M. Bosetti, P. Appendino, C. Vitale Brovarone, G. Maina and M. Cannas: *Biomaterials*, 2005, **26/25**, 5111–5119.
35. C. Moiescu, C. Jana and C. Russel: *J. Non-Cryst. Solids*, 1999, **248**, 169–175.
36. C. Moiescu, C. Jana, S. Hablitz, G. Carl and C. Russel: *J. Non-Cryst. Solids*, 1999, **248**, 176–182.
37. S. Di Nunzio and E. Verne: ‘Process for the production of silver-containing prosthetic devices’, patent no. WO2006/058906 A1.
38. T. Kokubo and H. Takadama: *Biomaterials*, 2006, **27**, 2907–2915.
39. G. M. Bruinsma, H.C. van der Mei and H. J. Busscher: *Biomaterials*, 2001, **22**, 3217–3224.
40. M. Quirynen, M. Marechal, H. J. Busscher, A. H. Weerkamp, J. Arends, P. L. Darius and D. van Steenberghe: *J. Dent. Res.*, 1989, **68**, (5), 796–799.
41. ‘Performance standards for antimicrobial disk susceptibility tests’, Approved Standard M2-A9, 9th edn, NCCLS, Villanova, PA, USA, 2003.
42. ‘Methods for dilution antimicrobial susceptibility tests for bacteria that grow aerobically’, Approved Standard M7-A6, 6th edn, NCCLS, Villanova, PA, USA, 2003.
43. R. R. Seghi, I. L. Denry and S. F. Rosenstiel: *J. Prosthet. Dent.*, 1995, **74**, (2), 145–150.
44. R. Martinetti and A. Nataloni: ‘Verifica Sperimentale del comportamento a frattura di un bioceramico impiantato nel tessuto osseo’, 2003, Faenza, FIN-CERAMICA FAENZA s.r.l.
45. J. L. Zhao, T. Fu, Y. Han and K. W. Xu: *Mater. Lett.*, 2004, **58**, (1–2), 163–168.